Archives of Biochemistry and Biophysics 537 (2013) 39–48

Contents lists available at SciVerse ScienceDirect

Archives of Biochemistry and Biophysics

journal homepage: www.elsevier.com/locate/yabbi

Enzymatic and structural characterization of hydrolysis of gibberellin A4 glucosyl ester by a rice β-D-glucosidase

Yanling Hua [a,b], Sompong Sansenya [a], Chiraporn Saetang [a], Shinji Wakuta [a,1], James R. Ketudat Cairns [a,*]

[a] School of Biochemistry and Chemistry, Institute of Science, Suranaree University of Technology, Nakhon Ratchasima 30000, Thailand
[b] The Center for Scientific and Technological Equipment, Suranaree University of Technology, Nakhon Ratchasima 30000, Thailand

ARTICLE INFO

Article history:
Received 15 May 2013
and in revised form 11 June 2013
Available online 26 June 2013

Keywords:
β-Glucosidase
Gibberellin glucosyl ester
Covalent intermediate
X-ray crystal structure
Transglycosylation

ABSTRACT

In order to identify a rice gibberellin ester β-D-glucosidase, gibberellin A4 β-D-glucosyl ester (GA_4-GE) was synthesized and used to screen rice β-glucosidases. Os3BGlu6 was found to have the highest hydrolysis activity to GA_4-GE among five recombinantly expressed rice glycoside hydrolase family GH1 enzymes from different phylogenic clusters. The kinetic parameters of Os3BGlu6 and its mutants E178Q, E178A, E394D, E394Q and M251N for hydrolysis of *p*-nitrophenyl β-D-glucopyranoside (*p*NPGlc) and GA_4-GE confirmed the roles of the catalytic acid/base and nucleophile for hydrolysis of both substrates and suggested M251 contributes to binding hydrophobic aglycones. The activities of the Os3BGlu6 E178Q and E178A acid/base mutants were rescued by azide, which they transglucosylate to produce β-D-glucopyranosyl azide, in a pH-dependent manner, while acetate also rescued Os3BGlu6 E178A at low pH. High concentrations of sodium azide (200–400 mM) inhibited Os3BGlu6 E178Q but not Os3BGlu6 E178A. The structures of Os3BGlu6 E178Q crystallized with either GA_4-GE or *p*NPGlc had a native α-D-glucosyl moiety covalently linked to the catalytic nucleophile, E394, which showed the hydrogen bonding to the 2-hydroxyl in the covalent intermediate. These data suggest that a GH1 β-glucosidase uses the same retaining catalytic mechanism to hydrolyze 1-*O*-acyl glucose ester and glucoside.

© 2013 Elsevier Inc. All rights reserved.

Introduction

Beta-glucosidases (β-D-glucopyranoside glucohydrolases, E.C. 3.2.1.21) are enzymes that hydrolyze the β-*O*-glycosidic bond at the anomeric carbon of a nonreducing terminal D-glucosyl moiety to release D-glucose from glycosides and oligosaccharides. These enzymes are found in essentially all living organisms and have been implicated in a diversity of roles, such as biomass conversion in microorganisms [1] and activation of defense compounds [2,3], phytohormones [4,5], lignin precursors [6], aromatic volatiles [7], and metabolic intermediates [8] by releasing glucose blocking groups from their inactive glucosides in plants. To achieve specificity for these various functions, different β-glucosidases must bind to distinct aglycones with a wide variety of structures, in addition to the glucose of the substrate.

β-Glucosidases have been classified into glycoside hydrolase (GH)[2] families GH1, GH3, GH5, GH9, GH30, and GH116, based on their amino acid sequences and structural similarity, while other β-glucosidases remain to be classified [9–12]. Most characterized plant β-glucosidases belong to GH1, which falls in GH Clan A, as do GH5 and GH30. GH Clan A enzymes have $(\beta/\alpha)_8$-barrel structures with catalytic acid/base and nucleophile on the ends of strands 4 and 7 of the barrel, respectively. The mechanism by which GH1 enzymes recognize and hydrolyze substrates with different specificities remains an area of intense study.

Among β-glucosidase functions in plants, the function of phytohormone activation has attracted many peoples' interest. Phytohormone glucosyl conjugates are ubiquitous in plants, including those of gibberellic acids (GAs), abscisic acid (ABA), cytokinins,

* Corresponding author. Address: Institute of Science, Suranaree University of Technology, 111 University Avenue, Nakhon Ratchasima 30000, Thailand. Fax: +66 44 224185.
E-mail address: cairns@sut.ac.th (J.R. Ketudat Cairns).
[1] Present address: Research Faculty of Agriculture, Hokkaido University, Kita-ku, Sapporo 062-8555, Japan.

[2] *Abbreviations used:* A_{405}, absorbance at 405 nm; ABA, abscisic acid; ABA-GE, ABA β-D-glucosyl ester; API-ES, atmospheric pressure ionization-electrospray; DAD, diode array detector; DMSO, dimethyl sulfoxide; DNP2FG, 2,4-dinitrophenyl-2-deoxy-2-fluoro-β-D-glucopyranoside; EtOAc, ethyl acetate; GA, gibberellic acid(s); GA_4-GE, gibberellin A4 β-D-glucosyl ester; G2F, 2-deoxy-2-fluoroglucoside; GH, glycoside hydrolase; IAA, indole acetic acid; IAA-GE, IAA β-D-glucosyl ester; IMAC, immobilized metal affinity chromatography; MeOH, Methanol; MES, 2-(N-morpholino)ethanesulfonic acid; NaOAc, sodium acetate; PEG5000MME, polyethylene glycol 5000 monomethyl ester; *p*NPG, *p*-nitrophenol; *p*NPGlc, *p*-nitrophenyl β-D-glucopyranoside; TEV, tobacco etch virus (protease).

0003-9861/$ - see front matter © 2013 Elsevier Inc. All rights reserved.
http://dx.doi.org/10.1016/j.abb.2013.06.005

auxins, and jasmonic acid derivatives, and β-glucosidases that hydrolyze these conjugates have been found in plants [4,13–20].

ABA and the auxin indole-3-acetic acid (IAA) have both been found as inactive 1-*O*-acyl glucose esters in plants. ABA is critical for plant growth, development, and adaptation to various stress conditions. Plants have to adjust ABA levels constantly to respond to changing physiological and environmental conditions [14]. Abscisic acid glucose ester (ABA-GE) is a biologically inactive form that constitutes a reserve form of ABA. Two *Arabidopsis* β-glucosidase (AtBG1 and AtBG2) were found to hydrolyze ABA-GE to form free ABA and to be essential to proper response to drought stress and delay in seed germination, despite the fact that other ABA-GE hydrolyzing enzymes were detected [14,17]. IAA glucosyl ester (IAA-GE) is also an inactive, stored form that can also be hydrolyzed by IAA-glucose hydrolase to release active IAA [15].

Both 1-*O*-acyl glucosyl esters and glucosides of GAs are found in plants. GAs promote germination, shoot elongation, and flower development, among their many functions [21]. It has been suggested that GA glucosyl esters are deactivated GAs that can be enzymatically reconverted to active GAs, thus serving as a reserve form of biologically active GAs [22]. After [^{13}C]GA_{20}-β-D-glucosyl ester was injected into light-grown maize seedlings, the metabolites, [^{13}C]GA_{20}, [^{13}C]GA_{29}, [^{13}C]GA_{20}-13-*O*-glucoside, [^{13}C]GA_{29}-2-*O*-glucoside, [^{13}C]GA_8 and [^{13}C]GA_8-2-*O*-glucoside were identified in the extracts of the seedlings made 24 h after the injection [23]. This showed that the endogenous hydrolysis of the introduced conjugate and its reconjugation led to the three new glucosides. In rice, [^{3}H]GA_1, [^{3}H]GA_2, [^{3}H]GA_{34}, the glucosides of [^{3}H]GA_2, [^{3}H]GA_4, [^{3}H]GA_8 and [^{3}H]GA_{34}, and the glucosyl ester of [^{3}H]GA_4 (GA_4-GE) have been found after application of [^{3}H]GA_4 to cell suspension cultures of *Oryza sativa* cv. nipponbare [24].

β-Glucosidases have been proposed to hydrolyze the GA conjugates to active GAs, but the molecular identification of these enzymes and investigation of their modes of action have yet to be reported. Schliemann [13] reported that β-glucosidases extracted from mature rice seeds and seedlings have different hydrolytic activities toward GA_8-2-*O*-glucoside, GA_3-3-*O*-glucoside and 1-*O*-GA_3-glucosyl ester, but he did not purify and characterize the β-glucosidases. Furthermore, the substrate specificity of β-glucosidase to GA conjugates and how β-glucosidase binds to GA conjugates has yet to be reported. In this study, we identified a rice GA_4-GE β-D-glucosidase and characterized its mechanism of glucosyl ester hydrolysis by comparing hydrolysis and transglycosylation activities of wild type and acid/base mutant enzymes with GA_4-GE. To better understand the ester-enzyme interaction, structures of mutant enzymes soaked with GA_4-GE and *p*NPGlc were also determined.

Materials and methods

Synthesis of GA_4-GE

GA_4-GE was synthesized from GA_4 (Jiangsu Fengyuan Bioengineering Co.Ltd, P.R. China) following the method of Hiraga, et al. [25]. The acetylated and deacetylated GA_4-GE were obtained with 43.7% and 40.5% yields, respectively. The synthesized acetylated and deacetylated GA_4-GE structures were confirmed by NMR spectra on a 300 MHz NMR spectrometer with a Varian 300 ID/PFG probe at a frequency of 299.986 MHz (Unity INOVA, Varian, USA). Deuterated chloroform ($CDCl_3$) and dimethyl sulfoxide-d_6 (DMSO-d_6) were used as solvents for acetylated and deacetylated GA_4-GE, respectively. The ^{1}H NMR was consistent with the published data for GA_4-GE [25].

The identity of the deacetylated GA_4-GE was also confirmed from its mass spectrum (data not shown). In the positive mode, we detected $[M+Na]^+$ at *m*/*z* 517.1, $[M+H-H_2O]^+$ at *m*/*z* 477.2, and $[M+H-Glc]^+$ at *m*/*z* 315.5.

Expression of rice GH1 enzymes to screen for GA_4-GE hydrolysis

Five GH1 enzymes that have been expressed in our laboratory, Os3BGlu6 [26], Os3BGlu7 [27], Os4BGlu12 [28], Os4BGlu18 (S. Baiya et al., unpublished) and Os9BGlu31 [29] were expressed as N-terminal thioredoxin fusion proteins in *Escherichia coli* and purified by immobilized metal affinity chromatography, as previously described. The purified fusion proteins were tested for the hydrolysis activity to *p*NPGlc and GA_4-GE according to the method described below.

Site-directed mutagenesis of Os3BGlu6

Mutagenesis of the pET32/Os3BGlu6 expression vector [26] to create the Os3BGlu6E178A, Os3BGlu6E178Q, Os3BGlu6E394D and Os3BGlu6E394Q mutations was performed with the QuikChange® Site-Directed Mutagenesis Kit (Stratagene, Agilent Corp., La Jolla, CA, USA) according to the supplier's instructions. The following oligonucleotides were used for mutagenesis: for E178A, 5′GATCACGCTCAACGCGCCGCACACGGTG3′ and its reverse complement; for E178Q, 5′GGATCACGCTCAACCAACCGCACACGGTGGC3′ and its reverse complement; for E394D, 5′CCAGTGTACATCACTG ATAACGGGATGGATGACAGC3′ and its reverse complement; and for E394Q, 5′CCACCAGTGTACATCACTCAGAACGGGATGGATGA-CAGC3′ and its reverse complement. The cDNA were confirmed to include the desired mutations and be free of additional mutations by automated DNA sequencing (Macrogen Corp., Rep. of Korea).

Recombinant expression and purification of the mutants of Os3BGlu6

The wild type rice Os3BGlu6 and its mutants M251N, E178Q, E178A, E394D and E394Q were expressed in *E. coli* strain Origami (DE3) as fusion proteins with N-terminal thioredoxin and His_6 tags as described previously for Os3BGlu6 [26]. The crude proteins were first purified by immobilized metal (Co^{2+}) affinity chromatography (IMAC). The N-terminal thioredoxin, His_6 and S tags were then excised with TEV protease, and removed with a second IMAC column purification. Protein concentrations were estimated by the Bradford protein assay (Bio-Rad) with bovine serum albumin as the standard. The values from this assay were in the good agreement with those obtained from the 280 nm absorbance with the calculated extinction coefficient.

Determination of pH optimum for Os3BGlu6 and its mutants

The optimum pH of Os3BGlu6 and Os3BGlu6 M251N hydrolysis of *p*NPGlc were determined by incubating 1 μg of enzyme with 2 mM *p*NPGlc in 80 μl of 100 mM universal buffer (citric acid-disodium hydrogen phosphate), pH 2.0–11.0 in 0.5-pH-unit increments, at 30 °C for 10 min. The reactions were stopped by adding 100 μl of 2 M sodium carbonate. The released *p*-nitrophenol (*p*NP) was quantified by measuring the absorbance at 405 nm (A_{405}) with a microplate reader (Thermo Labsystems, Finland) and comparing it to that of a *p*NP standard curve.

The optimum pH of Os3BGlu6 and its mutants M251N, E178Q and E178A for hydrolysis of GA_4-GE were determined by incubating 1 μg of Os3BGlu6 or Os3BGlu6 M251N, or 5.0 μg of E178Q or E178A with 0.86 mM GA_4-GE in 80 μl of 100 mM universal buffer, pH 2.0–11.0 in 0.5-pH-unit increments, at 30° for 20 min. The reactions were stopped by boiling 1 min and cooled on ice immediately. The released glucose was quantified with a glucose oxidase assay [27].

Measurement of wild type and mutant Os3BGlu6 activities for hydrolysis of GA_4-GE and pNPGlc

The activities of Os3BGlu6 wild type and mutants to hydrolyze *p*NPGlc were measured as described for the pH optimum determination, but in 50 mM sodium acetate (NaOAc) buffer, pH 5.0. To measure hydrolysis activities toward GA_4-GE, Os3BGlu6 wild type and M251N mutant enzymes were incubated with GA_4-GE in 50 mM NaOAc, pH 5.0, but 50 mM 2-(N-morpholino)ethanesulfonic acid (MES) buffer was selected for the E178Q and E178A mutants to avoid transglucosylation. For determination of kinetic parameters, variable reaction times, enzyme amounts and substrate concentrations were tested to obtain the initial velocities. The K_m and k_{cat} were calculated from nonlinear regression of Michaelis–Menten plots with Grafit 5.0 software (Erithacus Software, Horley, UK).

Identification of transglucosylation product with TLC, LC-MS and NMR

Transglucosylation reactions were studied for Os3BGlu6 wild type, M251N, E178Q and E178A mutants. 2 mM *p*NPGlc, 5 mM GA_4-GE or 2,4-dinitrophenyl-2-deoxy-2-fluoro-β-D-glucopyranoside (DNP2FG) donor was reacted with 1.0 μg of enzymes in 50 mM MES buffer, pH 5; and 40 mM sodium azide or 0.96 mM free GA_4 was used as acceptor. At different times, 10 μl aliquots of each reaction mix were removed, boiled 1 min, and kept on ice for TLC analysis. Reactions without enzymes were used as controls. Sample aliquots were spotted on TLC plates, which were developed with EtOAc–MeOH–H_2O (7.5:2.5:1.0) or $CHCl_3$–MeOH (7:3). The products were detected by staining with 10% sulfuric acid in ethanol followed by charring.

The new transglucosylation products of E178Q and E178A were analyzed by LC-MS. Samples were separated over a ZORBAX Eclipse XDB-C18 column (4.6 × 150 mm, 5 μm, Agilent, USA) on an Agilent 1100 HPLC. A gradient of 0–80% MeOH in 0.05% formic acid was run over 20 min at a flow rate of 0.8 ml/min. The ion peaks and mass spectra were detected with an Agilent single quadrupole MSD mass spectrometer with the atmospheric pressure ionization-electro spray (API-ES) source in negative and positive ion modes. The scan range was 100–1000 *m*/*z*, and the fragmentor voltage was 70 V. The VCap was 3000 V for both positive and negative modes.

The transglucosylation product was collected from HPLC separations and dried with a vacuum centrifuge. The product was dissolved in acetone-d_6, and ^{1}H NMR and gCOSY spectra were collected with a 300 MHz NMR spectrometer (Unity INOVA, Varian, USA).

Transglucosylation kinetics of the mutants of Os3BGlu6

The pH optima of E178Q and E178A for transglucosylation were determined in 50 mM MES, pH 5.0–7.5, and 50 mM sodium acetate, pH 4.0–6.0 in 0.5-pH-unit increments. Two micrograms of E178Q or E178A were incubated with 2 mM GA_4-GE and 100 mM sodium azide, in the different pH buffers at 30 °C for 30 min. The reactions without sodium azide were used to measure hydrolysis activities. The reactions were stopped by boiling 1 min and cooled on ice immediately. The reaction mixes were centrifuged at 6000 rpm for 15 min and separated on LC-MS, as described in the preceding section. The GA_4 released was detected with a diode array detector (DAD) at 210 nm, and the amounts were calculated by comparison of the peak areas to a GA_4 standard curve.

The concentrations of donor GA_4-GE and acceptor sodium azide were varied to test their effects on transglucosylation kinetics. The concentration of sodium azide was varied from 0 to 400 mM, while the GA_4-GE donor was fixed at 2 mM. The reactions were performed in 50 mM MES, pH 5, at 30 °C for 20 min. The turnover rates of GA_4 release per minute per unit enzyme (V_0/E_0) were calculated based on the GA_4 peak area. For the reactions varying the concentrations of GA_4-GE donor, sodium azide was fixed at 50, 100, 200 and 400 mM, and compared to reactions without sodium azide.

Crystallization of Os3BGlu6 E178Q

Purified Os3BGlu6 E178Q and Os3BGlu6 E394D were concentrated to 5 mg/ml and crystallized by hanging drop vapor diffusion with a precipitant of 13% polyethylene glycol 5000 monomethyl ester (PEG5000MME), 0.1 M Bis/Tris, pH 6.5, for Os3BGlu6 E178Q with *p*NPGlc and Os3BGlu6 E178Q with GA_4-GE, and 17% PEG5000MME, 0.1 M Bis/Tris, pH 6.5 for Os3BGlu6 E394D with GA_4-GE. The crystals were approximately 0.5 × 0.1 × 0.1 mm in size after growing 2 days. For cryo-protection, the crystals were transferred to a solution consisting of 22% PEG5000MME, 0.2 M Bis/Tris, pH 6.5, 18% (v/v) glycerol, which contained 10 mM GA_4-GE or *p*NPGlc.

X-ray diffraction data collection and processing

The data sets were collected at 100 K in a nitrogen stream (CryoJet; Oxford Instrument) on the PX 13B beamline at the National Synchrotron Radiation Research Center, Hsinchu, Taiwan, with a 1.0 Å wavelength X-ray beam and an ADSC Quantum 315 CCD detector. All the diffraction images were indexed, integrated and scaled with the HKL-2000 program [30]. The crystals of Os3BGlu6 E178Q soaked with GA_4-GE and *p*NPGlc belonged to the orthorhombic space group $P2_12_12_1$ and diffracted to 1.97 and 1.90 Å resolutions, respectively. Unit cell parameters for Os3BGlu6 E178Q with GA_4-GE were $a = 57.1$, $b = 91.2$, $c = 111.4$ Å, $\alpha = \beta = \gamma = 90°$, while those with *p*NPGlc were $a = 57.0$, $b = 91.1$, $c = 111.2$ Å, $\alpha = \beta = \gamma = 90°$ and for Os3BGlu6 E394D_GA_4-GE were $a = 56.5$, $b = 91.2$, $c = 111.2$ Å, $\alpha = \beta = \gamma = 90°$. Data-collection and processing statistics for the Os3BGlu6 E178Q complex structures are presented in Table 1.

Structure refinement

The structures of Os3BGlu6 E178Q with GA_4-GE or *p*NPGlc and Os3BGlu6 E394D with GA_4-GE were solved via rigid body refinement with the wild type Os3BGlu6 structure (PDB: 3GNO) as a template model. A subset of 5% of the structure factor amplitudes was reserved for R_{free} determination. Manual rebuilding of the model was performed in Coot [31] and refinement with REFMAC5 [32]. The occupancy of the glucose and glycerol in the active site of Os3BGlu6 E178Q with GA_4-GE was refined by setting the occupancy for the two moieties at values that added to 1.00 or less and minimizing the positive and negative densities around the ligands in the weighted Fo–Fc map, R_{free} and B-values. The glucose bound conformation of E394 (conformation A) was set at the same occupancy as the glucose, while the sum of the occupancies of the two E394 conformations was held at 1.00. The overall quality of each model was evaluated with the program PROCHECK [33]. Additional structure determination and refinement statistics are presented in Table 1. All the structure figures were drawn with PyMOL (Schrödinger, USA).

Results

GA_4-GE hydrolysis by recombinantly expressed rice GH1 enzymes

GA_4-GE, which has previously been reported in rice [24], was synthesized and used to screen GH1 enzymes for GA_4-GE hydroly-

Table 1
Data-collection and structure-refinement statistics.

Dataset	Os3BGlu6 E178Q *p*NPGlc	Os3BGlu6 E178Q GA_4-GE
PDB code	3WBA	3WBE
Beamline	BL13B1	BL13B1
Wavelength (Å)	1.00	1.00
Space group	$P2_12_12_1$	$P2_12_12_1$
Unit-cell parameters (Å)	a = 57.0	a = 57.1
	b = 91.1	b = 91.2
	c = 111.2	c = 111.4
Resolution range (Å)	30–1.90	30–1.97
Resolution outer shell(Å)	1.97–1.90	2.04–1.97
No. Unique reflections	46370	41777
No. Observed reflections	297256	297549
Completeness (%)	99.3 (100)	99.9 (100)
Average redundancy per shell	6.5 (6.3)	7.1 (7.2)
I/σ (I)	28.9 (4.5)	23.3 (6.6)
$R_{(merge)}$ (%)	6.0 (41.0)	8.4 (27.6)
R_{factor} (%)	14.8	14.5
R_{free} (%)	17.9	18.0
No. of residues in protein	478	478
No. Protein atoms	3917	3952
No. Ligand atoms	11 (Glc)	11 (Glc)
No. Other hetero atoms	36 (GOL)	36 (GOL)
No. waters	534	491
Mean B-factor	18.9	22.6
Protein	16.6	20.6
Ligand	12.1	11.1
Other hetero atoms	35.3 (GOL)	44.2 (GOL)
Waters	34.3	36.8
r.m.s. bond deviations (length)	0.013	0.013
r.m.s angle deviations (degrees)	1.290	1.264
Ramachandran plot		
Residues in most favorable regions (%)	88.9	88.6
Residues in additional allowed regions (%)	10.7	10.9
Residues in generously allowed regions (%)	0.5	0.5
Residues in disallowed regions (%)	0.0	0.0

sis activity. Five rice GH1 enzymes that have been expressed in *E. coli* were tested for the hydrolysis of *p*NPGlc and GA_4-GE. As shown in Table 2, Os3BGlu6 was found to have the highest hydrolysis activity to GA_4-GE among these enzymes. Although Os9BGlu31 had a higher ratio of activity toward GA_4-GE compared to *p*NPGlc (0.27 vs. 0.07 for Os3BGlu6), it is primarily a transglycosidase [29] and has low activity toward both substrates.

Hydrolysis activities of Os3BGlu6 and its mutants

Mutation of the putative catalytic acid/base and nucleophile residues and aglycone-binding residue M251 had differential effects on *p*NPGlc and GA_4-GE hydrolysis. The mutation of the Os3BGlu6 glutamate residue 178 to alanine (E178A) and glutamine (E178Q) and glutamate residue 394 to aspartate (E394D) and glutamine (E394Q) reduced the relative hydrolytic activity toward *p*NPGlc to <1%, while the M251N mutant reduced this activity to 52% (Table 3). The relative activity of M251N was 88.9% for GA_4-GE, and the catalytic efficiency (k_{cat}/K_m) followed the same pattern with decreases from 6.2 to 2.6 $mM^{-1}\ s^{-1}$ for *p*NPGlc, and from 0.13 to 0.08 $mM^{-1}\ s^{-1}$ for GA_4-GE compared to its wild type. For GA_4-GE, E178A had 22.2% and E178Q 12.5% of the relative hydrolytic activity of wild type Os3BGlu6 with both K_m and k_{cat} values lower than wild type. In contrast, the E394Q and E394D mutants had <2% wild type relative hydrolytic activity with GA_4-GE, similar to that with *p*NPGlc.

The Os3BGlu6 wild type and its M251N mutant were found to have high *p*NPGlc hydrolysis activity between pH 4.0 to 5.0, with the highest value at pH 4.5, while the activity dropped quickly above pH 5.5 (Supplementary data Fig. S1A). With GA_4-GE as substrate, Os3BGlu6 wild type and M251N, E178Q and E178A mutants all had highest hydrolytic activities at pH 4.5 (Supplementary data Fig. S1B). The activities of Os3BGlu6 E178Q and E178A dropped somewhat more slowly at pH above 6.0 compared to Os3BGlu6 wild type and M251N when hydrolyzing GA_4-GE, with 50% maximal activities at approximately 6.5 and 6.0, respectively.

Identification of transglucosylation product with azide

Previously, we found that Os3BGlu6 had negligible transglycosylation activity in reactions with alcohols, such as *n*-octyl alcohol, despite its hydrolytic activity toward the corresponding glycosides (S. Seshadri and J.R. Ketudat Cairns, unpublished). When we tested Os3BGlu6 for the ability to transfer glucose to azide and GA_4 acceptors in MES buffer, it hydrolyzed *p*NPGlc to *p*NP and glucose, and no transglucosylation products were observed. In contrast, the acid/base mutants Os3BGlu6 E178Q and E178A produced transglucosylation products with sodium azide and no significant hydrolysis products were detected in overnight reactions (Supplementary data Fig. S2). However, when the E178Q mutant was used in an attempt to generate GA_4-GE by transglycosylation of GA_4 acceptor with *p*NPGlc donor, no transglycosylation product was detected (data not shown). When GA_4-GE was used as donor and sodium azide as acceptor for Os3BGlu6 E178Q and E178A, a prominent transglucosylation product and a smaller amount of glucose were observed (Supplementary data Fig. S3).

The transglucosylation product of E178A with GA_4-GE was identified with LC-MS (Fig. 1). The peak of newly formed product at retention time 3.69 min had the molecular mass consistent with the 205.17 a.m.u mass of β-D-glucopyranosyl azide (1-azido-β-D-glucoside) expected from the retaining mechanism of the β-glucosidase [34]. Since formic acid (HCO_2H) was used in the mobile phase of LC-MS, its adduct ion $[M+HCO_2]^-$ was detected as the base peak along with $[M-H]^-$ and $[M+Cl]^-$ peaks (Supplementary data Fig. S4). The structure of the β-D-glucopyranosyl azide was also confirmed from its ^1H and gCOSY NMR spectra (data not shown). The ^1H spectrum peaks were assigned as: δ4.53, H1, d, $J_{2,1}$ = 9.0 Hz; δ3.85, H6, dd, $J_{6,6'}$ = 11.1 Hz; δ3.678, H6′, dd, $J_{5,6'}$ = 4.8 Hz, $J_{6,6'}$ = 11.1 Hz; δ3.364–3.458, H3, H4, H5, m; δ3.192, H2, t, $J_{1,2} = J_{3,2}$ = 9.0 Hz, which matched the published ^1H NMR data for β-D-glucopyranosyl azide [35]. The coupling constant between H1 and H2 of 9.0 Hz confirmed the β-D-glucopyranosyl azide had the "β" configuration.

Transglucosylation kinetics of the mutants of Os3BGlu6

The activity versus pH profiles for transglucosylation of azide with GA_4-GE donor were determined in sodium acetate and MES buffers (Supplementary data Fig. S5). For the Os3BGlu6 E178Q mutant, its optimum pH range was 5.0 to 6.0 in both buffers, slightly higher than its optimum pH for hydrolysis of GA_4-GE. The E178A mutant also had highest transglucosylation activity at pH 5.0 in the MES buffer, but was high at pH 4.0 in the sodium acetate. In the sodium acetate buffer, the release of *p*NP from *p*NPGlc by E178A was much higher than that in MES buffer, even without azide in the system.

Fig. 2 shows that when the concentration of donor GA_4-GE was fixed at 2 mM, the turnover rates, V_0/E_0, of GA_4 for Os3BGlu6 E178A slowly increased with increasing concentrations of sodium azide and reached its maximum at 400 mM sodium azide. However, for Os3BGlu6 E178Q, the turnover rates of GA_4 decreased at higher azide concentrations after reaching its maximum at 100 mM sodium azide. Since transglucosylation products were the main products and little glucose was evident when the azide acceptor was

Table 2
GA_4-GE hydrolysis by recombinantly expressed rice GH1 enzymes.

Enzyme	Phylogenetic cluster[a]	Activity toward GA_4-GE (μmol Glc released/min/mg)	Activity toward *p*NPGlc (μmol *p*NP released/min/mg)	Ratio of activity toward GA_4-GE/*p*NPGlc
Os3BGlu6	At/Os1	0.185	2.6	0.07
Os3BGlu7 (BGlu1)	At/Os4	0.02	4.0	0.005
Os4BGlu12	At/Os7	0.035	130	0.003
Os4BGlu18	At/Os5	N.D.	0.94	–
Os9BGlu31	At/Os6	0.02[b]	0.075[b]	0.27

N.D. means not detectable.
[a] Phylogenetic clusters from the eight sequence-based GH1 phylogenetic clusters shared by rice and Arabidopsis, as identified by Opassiri et al. [28].
[b] Activity is primarily transglycosylation, rather than hydrolysis [29].

present compared to when it was not, the parameters were calculated from the released GA_4 without subtracting hydrolysis. The Os3BGlu6 E179Q and E179A mutants had similar kinetic parameters for sodium azide in MES buffer, in the presence of 2 mM GA_4-GE with apparent K_m of 3.71 ± 0.47 mM, k_{cat} of 0.48 ± 0.01 s^{-1} and k_{cat}/K_m of 0.13 mM^{-1} s^{-1} for E178Q, and K_m of 3.1 ± 0.5 mM, k_{cat} of 0.204 ± 0.006 s^{-1}, and k_{cat}/K_m of 0.066 mM^{-1} - s^{-1} for E178A.

The effects of the concentration of sodium azide on the transglucosylation kinetics were further studied by measuring k_{cat} and K_m for GA_4-GE at 50, 100, 200 and 400 mM sodium azide (Table 4). For Os3BGlu6 E178Q, the K_m for GA_4-GE was >18-fold higher and k_{cat} at least 27-fold higher than that without sodium azide at all concentrations tested and both the K_m and k_{cat} increased with azide concentration, while the k_{cat}/K_m of GA_4-GE was highest at 0.51 mM^{-1} s^{-1} in 100 mM sodium azide and decreased to 0.41 and 0.29 when the concentration of sodium azide was increased to 200 and 400 mM, respectively. For Os3BGlu6 E178A, the K_m was 3-fold higher and k_{cat} 15-fold higher with 200 mM sodium azide compared to without sodium azide, while the k_{cat}/K_m of GA_4-GE was the same at 200 mM and 400 mM sodium azide.

Structure of Os3BGlu6E178Q soaked with either GA_4-GE or pNPGlc

When the Os3BGlu6 E178Q (acid/base) mutant was soaked with GA_4-GE, electron density for a glucosyl residue covalently bound to the catalytic nucleophile was seen, rather than a GA_4-GE molecule. However, when the glucosyl residue was built into the density, a patch of positive density protruded in the axial position from glucose carbon 4 and another positive density patch corresponded to the position of the E394 sidechain in the apo Os3BGlu6 structure (PDB: 3GNO). When the two sidechain positions and glucosyl moiety were set at 50% occupancy, a positive density defining a glycerol molecule was observed at positions overlapping the glucosyl C2, O2, C3, O3 and C4, but pointing away from O4. Thus, the glucose was present with partial occupancy, with a glycerol molecule from the solvent sharing the same positions as glucose carbons 2, 3 and 4 (PDB: 3WBE; Figs. 3B and 4B). The catalytic nucleophile was found in both the position previously seen for the covalent complex of Os3BGlu6 with 2-deoxy-2-fluoroglucoside (G2F) and that found in the apo enzyme (Figs. 3B, 4B, and 5C) [26]. Another crystal soaked in 2 mM *p*NPGlc also showed a covalently bound α-D-glucosyl residue, but with high occupancy (PDB: 3WBA; Figs. 3A and 4A). Since the structure appeared the same, but the ligand density was clearer in the *p*NPGlc structure (Fig. 4A), this structure best represents the covalent complex of the Os3BGlu6 E178Q mutant with an unmodified glucosyl residue. In both structures, the protein structure was well defined from G11 to T488, except for the loop of residues 331 to 337, which was poorly defined by the electron density, as was the N-terminus (similar to the previously reported wild type structure). Soaking of Os3BGlu6 E394D crystals with GA_4-GE resulted in electron density in both the glycone and aglycone subsites, but the occupancy was too low and the ligand density too poorly defined to build a reliable GA_4-GE complex structure.

In the covalent intermediate structure, the anomeric carbon of glucose is covalently bonded with Oε1 of E394 at a distance of 1.3 Å (Figs. 3A and 4A). The noncovalent interactions between the surrounding amino acids and the hydroxyls of the glucose ring, which took a $^4C_1$ chair conformation in the −1 subsite, included ten hydrogen bonds. The O2 atom of glucose forms hydrogen bonds with H132Nε2 (3.30 Å), N177 Oε1 (3.01 Å) and Q178Nε2 (2.99 Å), while O3 of glucose hydrogen bonds with Q31 Oε1 (2.66 Å) and W452Nε1 (2.85 Å). The glucosyl O4 is hydrogen bonded to Q31Nε2 (2.91 Å) and E451 Oε1 (2.61 Å), and O5 of glucose forms a hydrogen bond with Y321 (2.70 Å), while O6 forms a hydrogen bond with Oε2 of the same residue (2.60 Å). A water molecule (Water52) is also hydrogen bonded to O2 of glucose (2.80 Å) and E394 Oε1 (2.98 Å) (Fig 4A). A glycerol molecule was observed in the active site of this Os3BGlu6 E178Q structure in two conformations in the +1 subsite.

Discussion

Hydrolysis of GA_4-GE by Os3BGlu6 and its mutants

Thirty-four GH1 genes encoding potentially active rice β-glucosidases have been reported, and these were broken into eight sequence-based phylogenetic clusters that were shared between rice and *Arabidopsis thaliana* [28]. The five rice GH1 enzymes tested each represented a different phylogenetic cluster, from which we have been able to express active enzymes. Four of the tested enzymes had the ability to free GA_4 from GA_4-GE, and could potentially contribute to this release *in planta*. Although it also hydrolyzes β-1,2- and β-1,3-linked gluco-disaccharides and octyl-β-D-glucoside with high activity and may play other roles *in planta* [26], Os3BGlu6 had the highest activity toward GA_4-GE and was chosen to characterize the hydrolysis of the glucosyl ester.

Although much characterization has been done of the kinetics of hydrolysis of alkyl and aryl glycosides and oligosaccharides by β-D-glucosidases and their catalytic acid/base and nucleophile mutants [34–37], little description of the kinetics of glucosyl ester hydrolysis is available in the literature. Kiso et al. [38] compared the activities of 3 bacterial, 2 fungal and almond β-glucosidases for hydrolysis of 1-*O*-(*p*-hydroxybenzyoyl) β-D-glucose (pHBGlc), and found that *Caldocellum saccharolyticum* β-glucosidase had the highest activity of the commercial enzymes tested with 21% activity for pHBGlc relative to *p*NPGlc. Almond was reported to have approx. 5% relative activity for pHBGlc, somewhat less than the 7% of Os3BGlu6 for GA_4-GE compared to *p*NPGlc. In contrast to *Caldocellum saccharolyticum* and almond β-glucosidase, which had similar V_{max} for *p*NPGlc and *p*HBA but nearly 10-fold and 15-fold higher K_m for *p*HBA, respectively [39], Os3BGlu6 had similar K_m values for *p*NPGlc and GA_4-GE, but a 26-fold lower apparent k_{cat} for GA_4-GE relative to *p*NPGlc. Although the large aglycone of the GA_4-GE is not strictly comparable to that of *p*NPGlc, it shows that, in the case of Os3BGlu6, the rate of the hydrolysis and not the binding step is the distinguishing feature of the ester compare to the glucoside.

It might be expected that the relatively low pK_a of the leaving group would make the glucosyl ester relatively insensitive to the presence of a catalytic acid for the initial glycosylation step (the GA_4 pK_a is 4.3, compared to 7.2 for *p*NPGlc), similar to 2,4-dinitro-

Table 3
Hydrolysis activities of Os3BGlu6 and its mutants.

Enzyme	*p*NPGlc				GA_4-GE			
	Relative activity (%)	K_m (mM)	k_{cat} (s^{-1})	k_{cat}/K_m ($mM^{-1}\ s^{-1}$)	Relative activity (%)	K_m (mM)	k_{cat} (s^{-1})	k_{cat}/K_m ($mM^{-1}\ s^{-1}$)
Os3BGlu6	100	6.3 ± 0.4[a]	38.9 ± 0.9[a]	6.2[a]	100	5.8 ± 0.6	0.75 ± 0.04	0.13
Os3BGlu6-M251N	51.6	6.5 ± 0.7	15.4 ± 0.9	2.6	88.9	14.6 ± 2.0	1.2 ± 0.1	0.08
Os3BGlu6-E178Q	0.3	n.m.	n.m.	n.m.	12.5	0.09 ± 0.01	0.03 ± 0.001	0.33
Os3BGlu6-E178A	0.7	n.m.	n.m.	n.m.	22.2	3.7 ± 0.4	0.09 ± 0.005	0.03
Os3BGlu6- E394D	0.9	n.m.	n.m.	n.m.	1.4	n.m.	n.m.	n.m.
Os3BGlu6-E394Q	0.8	n.m.	n.m.	n.m.	0.6	n.m.	n.m.	n.m.

n.m.: not measured.
For the relative activity with *p*NPGlc, 0.5 μg of Os3BGlu6 wild type or M251 N, or 3 μg of E178A, E178Q, E394D or E394Q was incubating with 4 mM *p*NPGlc in NaOAc, pH 4.5 (final volume 50 μl) at 30 °C for 10 min. For the relative activity with GA_4-GE, 1.0 μg of Os3BGlu6 wild type or M251 N, or 3 μg of E178A, E178Q, E394D or E394Q was incubated with 1.7 mM GA_4-GE in NaOAc, pH 4.5 (final volume was 50 μl), at 30 °C for 20 min. The relative activities were calculated based on A_{405} and the amount of the enzymes. For determination of the kinetic parameters, 50 mM NaOAc buffer was used for Os3BGlu6 wild type and M251 N, for both substrates, but 50 mM MES buffer was selected for the E178Q and E178A mutants.
[a] Data from Seshadri et al. (2009).

phenyl glycosides [34,41], but other influences of having the ester bond in apposition to the glycosidic bond are not so clear. The Os3BGlu6 wild type had an optimum pH for hydrolysis of both *p*NPGlc and GA_4-GE at pH 4.5, indicating that the low pK_a of the leaving group carboxylate did not affect the pH optima. Although the Os3BGlu6 E178Q and E178A mutants had low activities toward *p*NPGlc, their GA_4-GE hydrolysis activities were significant and dropped slowly above pH 6.0, compared to wild type Os3BGlu6, consistent with their designations as catalytic acid/base mutants. The pH dependence of enzymatic reactions is generally considered to reflect ionizations of acid/base groups involved in catalysis [39,40]. The Os3BGlu6 E178Q and E178A mutants lack the ionizable group to donate a proton in the glycosylation step or extract a proton in the deglycosylation step, resulting in lower pH dependence at high pH.

In contrast to the Agrobacterium and rice Os3BGlu7 β-glucosidases [37,41], the acid/base glutamate to alanine (E178A) mutant was more active than the acid/base to glutamine mutant (E178Q). This was evidently due to the buildup of an intermediate on the enzyme, since both the K_m and k_{cat} dropped dramatically in the E178Q mutant. The X-ray crystallographic structure (Fig. 3) indicated this intermediate was the covalent intermediate formed in the glycosylation half reaction (Fig. 5). The glutamine sidechain can provide a hydrogen bond to stabilize the leaving group in glycosylation and acceptor in deglycosylation of the enzyme, giving it higher activity [42], but it evidently could not facilitate water as an acceptor in Os3BGlu6. Without E178, the low pK_a of GA_4 allows it to be released in the glycosylation step without general acid-assistance more effectively than *p*NPGlc, for which glycosylation appeared to be the rate-limiting step. The lack of deprotonation of the water molecule in the deglycosylation step makes Os3BGlu6 E178A and Os3BGlu6 E78Q relatively effective at transglycosylation with GA_4-GE donor compared to their wild type.

When the structure of wild type Os3BGlu6 was resolved by X-ray crystallography, the M251 residue was suggested to block binding of straight cellooligosaccharides in the active site cleft [26]. The mutation of M251 to asparagine resulted in 9 to 24-fold increases hydrolysis efficiency for oligosaccharides in Os3BGlu6 M251N compared to wild type [43]. So, it was of interest to see whether this mutation would affect the hydrolysis of less polar substrates like *p*NPGlc and GA_4-GE as well. The catalytic efficiencies (k_{cat}/K_m) for M251N were reduced 2.4-fold for *p*NPGlc, and 1.6-fold for GA_4-GE compared to wild type. The K_m to *p*NPGlc for both Os3BGlu6 and Os3BGlu6 M251N is almost the same, and the smaller k_{cat} of Os3BGlu6 M251N is the main cause for its lower k_{cat}/K_m compared to the wild type. In contrast, for GA_4-GE, the higher K_m for Os3BGlu6 M251N is the main reason for its lower k_{cat}/K_m compared to the wild type, suggesting that the larger aglycone of GA_4-GE may interact with residue M251, which may stabilize binding of large hydrophobic aglycones.

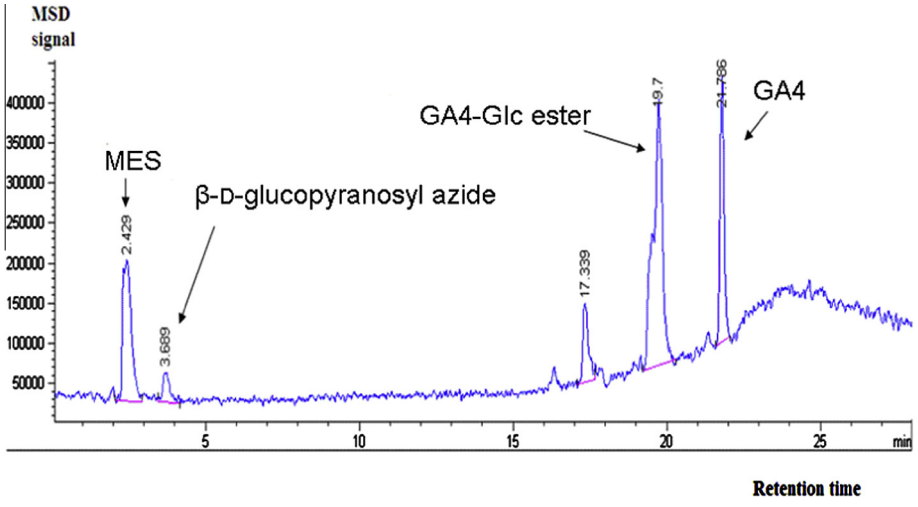

Fig. 1. The LC-MS chromatogram of the transglucosylation reaction of Os3BGlu6 E178A with GA_4-GE as donor and sodium azide as acceptor. The reaction components were separated by C18 reverse phase HPLC, as described in the methods. The detector was an Agilent MSD single quadrupole mass spectrometer with API-ES source in negative ion mode, with a scan range of 50–800 *m/z*.

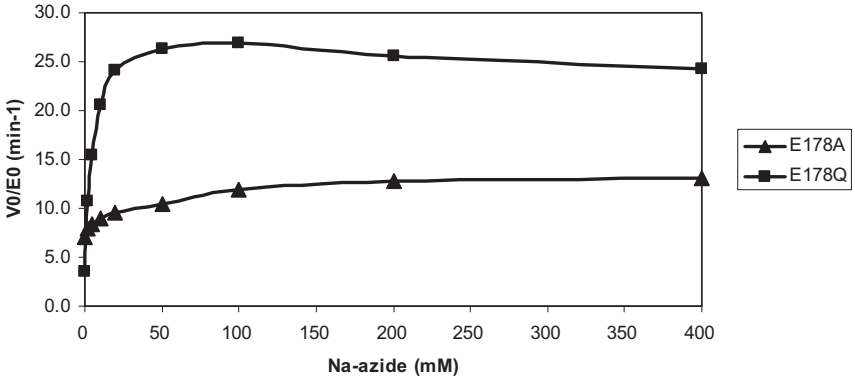

Fig. 2. Rates of transglucosylation of azide acceptor with GA_4-GE donor by the Os3BGlu6 E178A and E178Q acid/base mutants. The concentrations of sodium azide acceptor were varied from 0 to 400 mM, while donor GA_4-GE was fixed at 2 mM. The reactions were performed in 50 mM MES, pH 5, at 30 °C for 20 min. The turnover rates V_0/E_0 of GA_4 (μmole of GA_4 release per minute per μmole of enzyme) were calculated based on the area of GA_4 HPLC peaks. The total area of GA_4 was used without subtracting the hydrolysis reaction.

Table 4
Transglucosylation kinetics of Os3BGlu6 E178Q and Os3BGlu6 E178A for GA_4-GE donor at various fixed concentrations of sodium azide acceptor.

Enzyme	Sodium azide (mM)	K_m (mM)	k_{cat} (s^{-1})	k_{cat}/K_m ($mM^{-1}s^{-1}$)
Os3BGlu6 E178Q	0	0.09 ± 0.01	0.03 ± 0.001	0.33
	50	1.64 ± 0.15	0.81 ± 0.04	0.49
	100	1.69 ± 0.13	0.86 ± 0.04	0.51
	200	2.07 ± 0.31	0.84 ± 0.08	0.41
	400	3.97 ± 0.65	1.16 ± 0.14	0.29
Os3BGlu6 E178A	0	3.7 ± 0.4	0.09 ± 0.005	0.03
	200	11.6	1.39	0.12
	400	13.36	1.56	0.12

The transglucosylation rates were calculated from the released GA_4 without subtracting hydrolysis product.

Transglucosylation activities of Os3BGlu6E178Q and Os3BGlu6E178A

When azide was included in the reaction, both Os3BGlu6 E178A and E178Q could catalyze transglycosylation reactions from GA_4-GE to produce β-D-glucosyl azide, as shown schematically in Fig. 5. In this case, Os3BGlu6 E178Q had higher activity than E178A. For the Os3BGlu6 E178A, the GA_4 releasing activity in sodium acetate was much higher than that in MES buffer, even without azide in the system, indicating that acetate may also act as a nucleophile and/or substitute acid/base to rescue the activity, as was seen in the work of Wang et al. [35].

The transglucosylation turnover rate, V_0/E_0, of GA_4 increased very significantly as the concentration of azide was increased. The rate increase with increasing concentration of azide was also observed by Wang et al. [35]. They concluded that addition of azide as a competitive nucleophile increased k_{cat} values 100–300 fold for substrates for which the rate-limiting step is deglycosylation, such as GA_4-GE with Os3BGlu6 E178Q and Os3BGlu6 E178A. As the concentration of azide is increased, the rate of deglycosylation increases, until glycosylation becomes rate determining. The build-up at the E178Q covalent intermediate was released by reaction with the azide, which was apparently facilitated by interaction of Q178 with the azide. Although the K_m values for azide for the

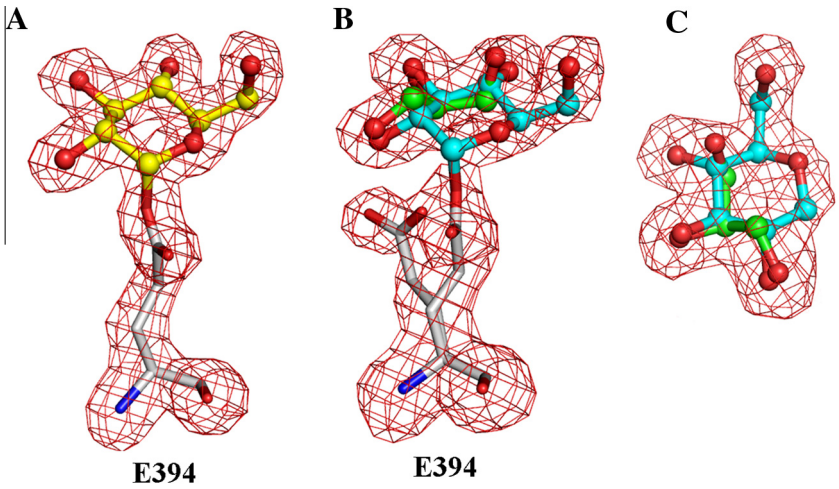

Fig. 3. The electron density map (Omit $F_{obs} - F_{calc}$ contoured at 3σ) of glycosyl-enzyme intermediate of the Os3BGlu6 E178Q with *p*NPGlc (A) and GA_4-GE (B). (A) The glucose of Os3BGlu6 E178Q soaked with *p*NPGlc are represented by balls and sticks with carbon in yellow for glucose. The nucleophile residue (E394) is represented by sticks with carbon in gray, oxygen in red and nitrogen in dark blue. (B) The mixed structures of apo Os3BGlu6 E178Q and Os3BGlu6 E178Q covalently bound to Glc from GA_4-GE was modeled with two conformations of E394 and glucose and glycerol occupying the same position, by refining the occupancy to 0.5 for glucose and glycerol and each of the E394 conformations. The glucose and glycerol are shown in ball and stick representation with carbon in cyan for glucose and in green for glycerol. The nucleophile residue (E394) is represented as sticks with carbon in gray, oxygen in red and nitrogen in dark blue. (C) A top view of the glucosyl ring and the overlapping glycerol electron density for Os3BGlu6 E178Q with GA_4-GE shown in B to clarity the different positions of the glucosyl 4-OH and glycerol 3-OH. (For interpretation of the references to colour in this figure legend, the reader is referred to the web version of this article.)

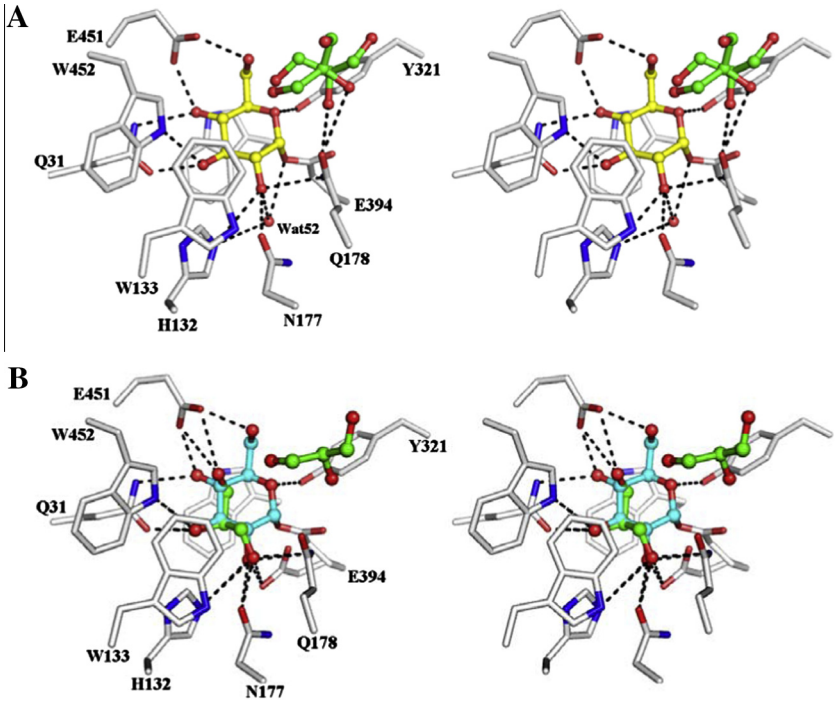

Fig. 4. Binding of glucose in the active site of Os3BGlu6 E178. A and B, Stereo view of protein–ligand interaction in the active site of the Os3BGlu6 E178Q soaked with *p*NPGlc and with GA_4-GE, respectively. The amino acids surrounding the −1 subsite are represented as sticks with carbon in gray, nitrogen in dark blue and oxygen in red. The covalent glucosyl moiety is represented as balls and sticks with carbon in yellow for Os3BGlu6 E178Q soaked with *p*NPGlc and in cyan for Os3BGlu6 E178Q soaked with GA_4-GE, and oxygen in red. The two glycerols in both complex structures are represented as balls and sticks with carbon in green and oxygen in red. Hydrogen bonding interactions of glucose and glycerol with amino acid residues are shown as black dotted lines.

two mutants were similar, the k_{cat}/K_m values for sodium azide as acceptor with 2 mM GA_4-GE donor of 0.13 mM^{-1} s^{-1} for Os3BGlu6 E178Q and 0.066 mM^{-1} s^{-1} for Os3BGlu6 E178A indicate that the polar glutamine at residue 178 in Os3BGlu6 E178Q supports transglycosylation by azide better than the nonpolar alanine residue in Os3BGlu6 E178A. A stronger interaction with the azide in the Os3BGlu6 E178Q mutant is also supported by the fact that it is inhibited by high concentrations of azide, while the E178A mutant is not.

Structures of Os3BGlu6 covalent intermediate complexes

Although we intended to obtain a noncovalent GA_4-GE complex with an Os3BGlu6 mutant, the high reactivity of this substrate resulted in poor density in the E394D nucleophile mutant active site and the covalent glucosyl-enzyme intermediate in the E178Q acid/base mutant. Fig. 6 shows that the positions and interactions made by amino acid residues surrounding the native glucosyl moiety in the active site of Os3BGlu6 E178Q with glucose from GA_4-GE

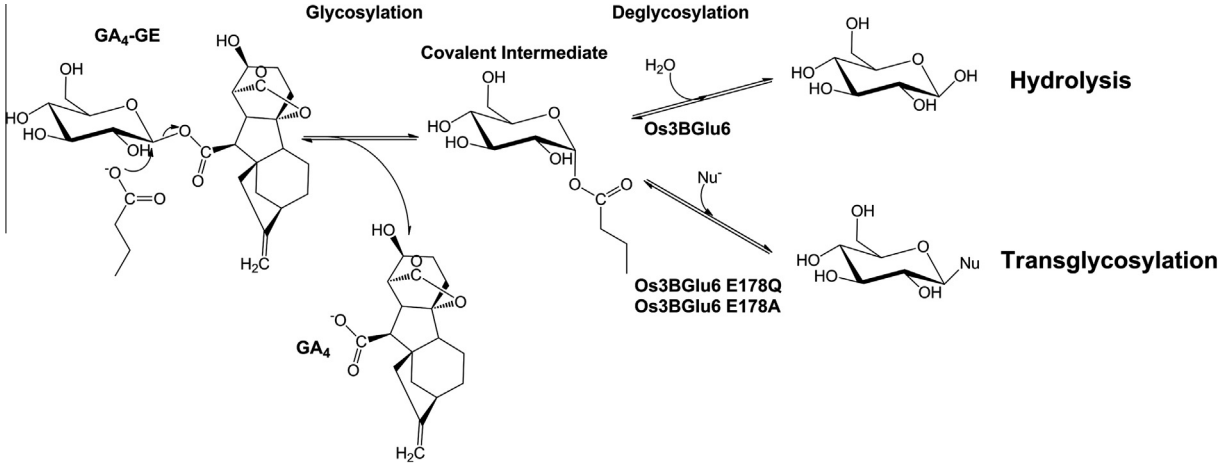

Fig. 5. Schematic of the hydrolysis and transglycosylation reactions catalyzed by Os3BGlu6 and its acid/base mutants with GA_4-GE. The first step, glycosylation, is allowed to proceed without acidic assistance to release the GA_4, due to its low pK_a. The covalent intermediate, seen in the crystal structures, builds up in the acid/base mutants E178A and E178Q, but the presence of a small nucleophile (Nu^-) such as azide promotes deglycosylation of the mutant enzymes by transglycosylation. In contrast, the wild type Os3BGlu6 only appears to catalyze hydrolysis.

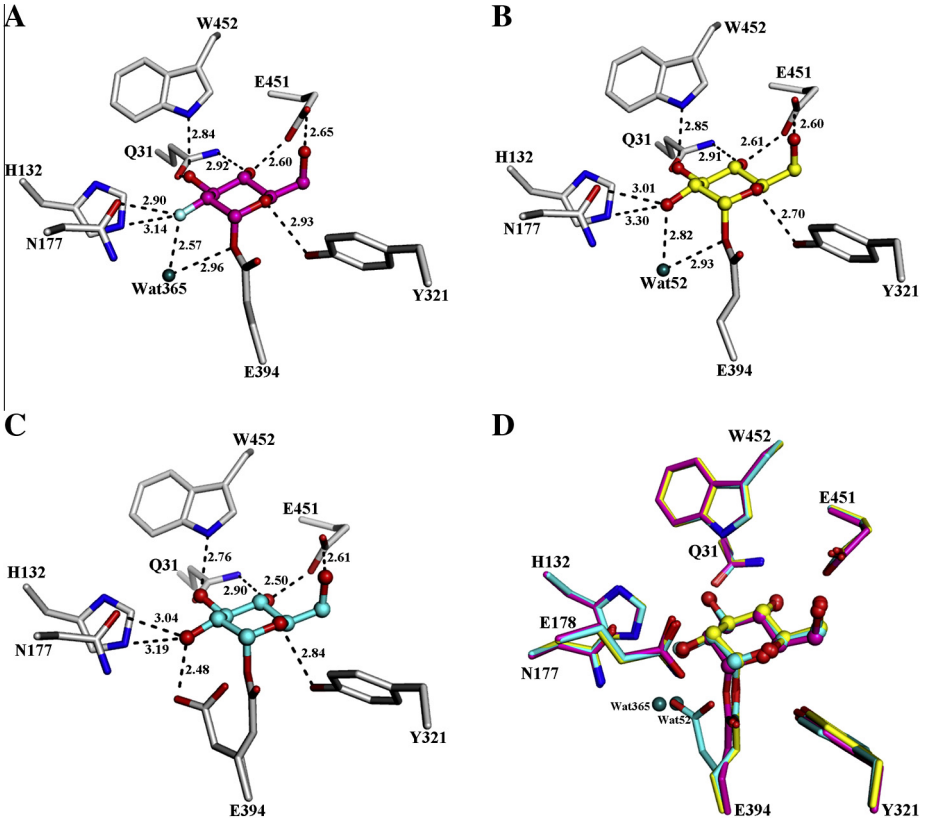

Fig. 6. Comparison of the active site region of Os3BGlu6 bound with G2F (A) and those of the structures of Os3BGlu6 E178Q soaked with *p*NPGlc (B) and Os3BGlu6 E178Q soaked with GA_4-GE (C). The G2F and glucosyl moieties are represented as balls and sticks with carbon in pink for G2F, in yellow for Os3BGlu6 E178Q soaked with *p*NPGlc and cyan for Os3BGlu6 E178Q soaked with GA_4-GE, oxygen in red and fluorine in pale cyan. The amino acid residues surrounding the ligands are represented by sticks with carbons in gray, nitrogens in dark blue and oxygens in red for all three structures. (D) Superpositioin of the three structures in (A–C), showing the nucleophile residues covalently bound to the glucosyl moiety at the −1 subsite of the Os3BGlu6E178Q structures soaked with *p*NPGlc (yellow carbons) and GA_4-GE_(cyan carbons) and to the G2F moiety in Os3BGlu6 (3GNP, pink carbons). The unbound position of the nucleophile is represented by the alternative conformation of Os3BGlu6 E178Q soaked with GA_4-GE. The molecules are represented as in (A–C), except for the protein carbon colors.

(PDB: 3WBE) or *p*NPGlc (PDB: WBA) were similar to those interacting with the 2-deoxyl-2-fluroglucopyranoside residue (G2F) in the structure of wild type Os3BGlu6 with G2F (3GNR). In the structure of Os3BGlu6/G2F complex [26], the density of the 2-deoxy-2-fluoroglucosyl residue matched a relaxed $^4C_1$ chair conformation, as did the glucosyl moiety in the Os3BGlu6 E178Q covalent intermediate structure (Fig 6D). The distance between the anomeric carbon of glucose and the Glu394 nucleophile residue of Os3BGlu6 E178Q was also similar to that in the G2F covalent complex (1.3 Å). A water molecule was observed between the 2-OH of glucose or fluorine atom of G2F and N177 and E394 in the Os3BGlu6 E178Q/Glc and Os3BGlu6/G2F structures. A water molecule in this position has been shown to be critical for the hydrolysis and glycosynthase reactions of Os3BGlu7 [43]. The hydrogen bonding pattern between glucosyl residues at the −1 subsite of the Os3BGlu6 E178Q/Glc covalent complex structure is similar when compared to that of the Os3BGlu6/G2F complex (Fig. 6A, B and C). The average distances between the 2-OH of the glucose and 2-fluorine of G2F moieties and polar atoms of the surrounding amino acid residues are similar (Fig 6A–D).

Many structures of GH1 glycosyl-enzyme intermediates with a 2-deoxy-2-fluoroglucosyl (G2F) moiety bound to the nucleophilic residue have been reported, including one for Os3BGlu6 (PDB code 3GNR) [26,44–49]. These GH1 glycosyl-enzyme intermediates used 2,4-dinitrophenyl 2-deoxy-2-fluoroglucoside, with which the substitution of an electronegative fluorine atom for a hydroxyl group adjacent to the reaction center at C-2 destabilizes the transition states and decreases the rates of both glycosylation and deglycosylation [50]. The human cytosolic β-glucosidase acid/base mutant glucose complex (2ZOX) is the only previously reported GH1 structure with the nucleophile covalently bound to native glucose [51]. The hydrogen bonding pattern between G2F molecule and the enzyme at the −1 subsite is conserved in other reported GH1 covalent intermediates, but this pattern lacks the hydrogen bonds for which the 2-OH is the proton donor seen in human cytosolic β-glucosidase and Os3BGlu6 E178Q covalent glucoside complex structures. In general, the reports of G2F complexes do not report hydrogen bonds to the 2-F group, but the conservation of the water in proximity to the fluorine in these complexes supports the idea that the fluorine may accept a hydrogen bond from the water and other nearby hydrogen donors. On the other hand, the loss of possible hydrogen bonds from the 2-OH to Oδ of N177 and Oε2 of E394 in Os3BGlu6, which are seen in the native glucosyl-enzyme intermediates (Fig. 6), may result in a further loss of stabilization of the transition state in the 2-F-glucoside reaction [51].

Conclusion

This work identified Os3BGlu6 as a β-glucosidase with relatively high activity to hydrolyze GA_4-GE. Comparison of the activity of Os3BGlu6 and its acid/base mutants, E178Q and E178A, for hydrolysis of *p*NPGlc and GA_4-GE suggested that hydrolysis of esters and glycosides is similar and the low pK_a of the carboxyl leaving group is what differentiates it, although the rate of the wild type enzyme is much slower with the ester. Despite the observation of little or no transglucosylation activity for wild type

Os3BGlu6, its acid/base mutants were still rescued by azide transglycosylation to form β-D-glucosyl azide. The covalent intermediate of Os3BGlu6 E178Q with unmodified α-D-glucoside was observed with either *p*NPGlc or GA_4-GE donor substrate, supporting the covalent double displacement mechanism for this enzyme with either glycoside or glycosyl ester substrates.

Acknowledgments

The authors are grateful to Assist. Prof. Dr. Thanaporn Manyum for providing her laboratory for initial synthesis work and Ms. Supaporn Baiya for providing Os4BGlu18 β-glucosidase. Suranaree University of Technology (SUT) and the Center for Scientific and Technological Equipment (CSTE) are thanked for supporting YH in her Ph.D. studies. The research funding was provided by SUT and the National Research University Project of the Commission on Higher Education of Thailand, along with the Thailand Research Fund (Grant BRG5380017).

Appendix A. Supplementary data

Supplementary data associated with this article can be found, in the online version, at http://dx.doi.org/10.1016/j.abb.2013.06.005.

References

[1] T. Fowler, in: A. Esen (Ed.), Biochemistry and Molecular Biology, American Chemical Society, Washington, DC, 1993, pp. 56–65. ACS Symposium Series 533.
[2] J.E. Poulton, Plant Physiol. 94 (1990) 401–405.
[3] L. Duroux, F.M. Delmotte, J.M. Lancelin, G. Keravis, C. Jay-Alleand, Biochem. J. 333 (1998) 275–283.
[4] B. Brzobohatý, I. Moore, P. Kristoffersen, L. Bako, N. Campos, J. Schell, K. Palme, Science 262 (1993) 1051–1054.
[5] A. Falk, L. Rask, Plant Physiol. 108 (1995) 1369–1377.
[6] D.P. Dharmawardhana, B.E. Ellis, J.E. Carlson, Plant Physiol. 107 (1995) 331–339.
[7] M. Reuveni, Z. Sagi, D. Evnor, A. Hetzroni, Plant Sci. 147 (1999) 19–24.
[8] L. Barleben, X. Ma, J. Koepke, G. Peng, H. Michel, J. Stöckigt, Biochim. Biophys. Acta. 1747 (2005) 89–92.
[9] B. Henrissat, Biochem. J. 280 (1991) 309–316.
[10] B.L. Cantarel, P.M. Coutinho, C. Rancurel, T. Bernard, V. Lombard, B. Henrissat, Nucleic. Acids Res. 37 (2009) D233–D238.
[11] J.R. Ketudat Cairns, A. Esen, Cell. Mol. Life Sci. 67 (2010) 3389–3405.
[12] B. Cobucci-Ponzano, V. Aurilia, G. Riccio, B. Henrissat, P.M. Coutinho, A. Strazzulli, A. Padula, M.M. Corsaro, G. Pieretti, G. Pocsfalvi, I. Fiume, R. Cannio, M. Rossi, M. Moracci, J. Biol. Chem. 285 (27) (2010) 20691–20703.
[13] W. Schliemann, J. Plant Physiol. 116 (1984) 123–132.
[14] K.H. Lee, H.L. Piao, H.Y. Kim, S.M. Choi, F. Jiang, W. Hartung, I. Hwang, J.M. Kwak, I.J. Lee, I. Hwang, Cell 126 (2006) 1109–1120.
[15] K. Kai, K. Wakasa, H. Miyagawa, Phytochemistry 68 (2007) 2512–2522.
[16] S. Wakuta, S. Hamada, H. Ito, H. Matsuura, K. Nabeta, H. Matsui, Phytochemistry 71 (2010) 1280–1288.
[17] Z.Y. Xu, K.H. Lee, T. Dong, J.C. Jeong, J.B. Jin, Y. Kanno, D.H. Kim, S.Y. Kim, M. Seo, R.A. Bressan, D.J. Yun, I. Hwang, Plant Cell 24 (2012) 2184–2199.
[18] Y. Koda, E.A. Omer, T. Yoshihara, H. Shibata, S. Sakamura, Y. Okazawa, Plant Cell Physiol. 29 (1988) 1047–1051.
[19] T. Yoshihara, M. Amanuma, T. Tsutsumi, Y. Okumura, H. Matsuura, A. Ichihara, Plant Cell Physiol. 37 (1996) 586–590.
[20] S. Wakuta, S. Hamada, H. Ito, R. Imai, H. Mori, H. Matsuura, K. Nabeta, H. Matsui, J. Appl. Glycosci. 58 (2011) 67–70.
[21] P.J. Davies, Plant Hormones: Physiology, Biochemistry and Molecular Biology, Kluwer Academic Publishes, 1995.
[22] G. Schneider, in: A. Crazier (Ed.), The Biochemistry and Physiology of Gibberellins, vol. 1, Praeger Publishers, New York, 1983, pp. 389–456.
[23] G. Schneider, E. Jensen, C.R. Spray, B.O. Phinney, Proc. Natl. Acad. Sci. USA 89 (1992) 8045–8048.
[24] M. Koshioka, E. Minami, H. Saka, R.P. Pharis, L.N. Mander, Gibberellins, Springer, New York, 1991. 264–272.
[25] K. Hiraga, T. Yokota, N. Takahashi, Phytochemistry 13 (1974) 2371–2376.
[26] S. Seshadri, T. Akiyama, R. Opassiri, B. Kuaprasert, J.R. Ketudat Cairns, Plant Physiol. 151 (1) (2009) 47–58.
[27] R. Opassiri, J.R. Ketudat Cairns, T. Akiyama, O. Wara-aswapati, J. Svasti, A. Esen, Plant Sci. 165 (2003) 627–638.
[28] R. Opassiri, B. Pomthong, T. Onkoksoong, T. Akiyama, A. Esen, J.R. Ketudat Cairns, BMC Plant Biol. 6 (2006) 33.
[29] S. Luang, J.-I. Cho, B. Mahong, R. Opassiri, T. Akiyama, K. Phasai, J. Komvongsa, N. Sasaki, Y. Hua, Y. Matsuba, Y. Ozeki, J.-S. Jeon, J.R. Ketudat Cairns, J. Biol. Chem. 288 (2013) 10111–10123.
[30] Z. Otwinowski, W. Minor, Meth. Enzymol. 276, Academic Press, New York, (1997) 307–326.
[31] P. Emsley, K. Cowtan, Acta Crystallogr. D 60 (2004) 2126–2132.
[32] G.N. Murshudov, A.A. Vagin, E.J. Dodson, Acta Crystallogr. D 53 (1997) 240–255.
[33] R.A. Laskowski, M.W. MacArthur, D.S. Moss, J.M. Thornton, Appl. Cryst. 26 (1993) 283–291.
[34] Q. Wang, D. Trimbur, R. Graham, R.A.J. Warren, S.G. Withers, Biochemistry 34 (1995) 14554–14562.
[35] Q. Wang, R.W. Graham, D. Trimbur, R.A.J. Warren, S.G. Withers, J. Am. Chem. Soc. 116 (1994) 11594–11595.
[36] L. Mackenzie, G. Sulzenbacher, C. Divne, T.A. Jones, H.F. Woldike, M. Schulein, S.G. Withers, G. Davies, Biochem. J. 335 (1998) 409–416.
[37] W. Chuenchor, S. Pengthaisong, R.C. Robinson, J. Yuvaniyama, J. Svasti, J.R. Ketudat Cairns, J. Struct. Biol. 173 (2011) 169–179.
[38] T. Kiso, S. Kitahata, K. Okamoto, S. Miyoshi, H. Nakano, J. Biosci. Bioeng. 90 (2000) 614–618.
[39] J.B. Kempton, S.G. Withers, Biochemistry 31 (1992) 9961–9969.
[40] L.P. McIntosh, G. Hand, P.E. Johnson, M. Joshi, M. Korner, L.A. Plesniak, L. Ziser, W.W. Wakarchuk, S.G. Withers, Biochemistry 35 (1996) 9958–9966.
[41] J. Müllegger, M. Jahn, H.M. Chen, R.A. Warren, S.G. Withers, Protein Eng. Des. Sel. 18 (2005) 33–40.
[42] S. Sansenya, J. Maneesan, Carbohydr. Res. 351 (2012) 130–133.
[43] J. Wang, S. Pengthaisong, J.R. Ketudat Cairns, Y. Liu, Biochim. Biophys. Acta. 1834 (2013) 536–545.
[44] W. Burmeister, S. Cottaz, H. Driguez, R. Iori, S. Palmieri, B. Henrissat, Structure 5 (1997) 663–675.
[45] P. Isorna, J. Polaina, L. Latorre-García, F.J. Cañada, B. González, J. Sanz-Aparicio, J. Mol. Biol. 371 (2007) 1204–1218.
[46] T.M. Gloster, S. Roberts, V.M.A. Ducros, G. Perugino, M. Rossi, R. Hoos, M. Moracci, A. Vasella, G.J. Davies, Biochemistry 43 (2004) 6101–6109.
[47] D.L. Zechel, S.P. Reid, D. Stoll, O. Nashiru, R.A. Warren, S.G. Withers, Biochemistry 42 (2003) 7195–7204.
[48] W. Chuenchor, S. Pengthaisong, R.C. Robinson, J. Yuvaniyama, W. Oonanant, D.R. Bevan, A. Esen, C.J. Chen, R. Opassiri, J. Svasti, J.R. Ketudat Cairns, J. Mol. Biol. 377 (2008) 1200–1215.
[49] S. Sansenya, R. Opassiri, B. Kuaprasert, C.J. Chen, J.R. Ketudat Cairns, Arch. Biochem. Biophys. 510 (2011) 62–72.
[50] J. Noguchi, Y. Hayashi, Y. Baba, N. Okino, M. Kimura, M. Ito, Y. Kakuta, Biochem. Biophys. Res. Commun. 374 (2008) 549–552.
[51] B. Rempel, S. Withers, Glycobiology 18 (2008) 570–586.